

Spectrum of confining strings in $SU(N)$ gauge theories

Luigi Del Debbio

Dipartimento di Fisica dell'Università di Pisa and I.N.F.N., I-56127 Pisa, Italy
E-mail: ldd@df.unipi.it

Haralambos Panagopoulos

Department of Physics, University of Cyprus, Nicosia CY-1678, Cyprus
E-mail: haris@ucy.ac.cy

Paolo Rossi

Dipartimento di Fisica dell'Università di Pisa and I.N.F.N., I-56127 Pisa, Italy
E-mail: rossi@df.unipi.it

Ettore Vicari

Dipartimento di Fisica dell'Università di Pisa and I.N.F.N., I-56127 Pisa, Italy
E-mail: vicari@df.unipi.it

ABSTRACT: We study the spectrum of the confining strings in four-dimensional $SU(N)$ gauge theories. We compute, for the $SU(4)$ and $SU(6)$ gauge theories formulated on a lattice, the string tensions σ_k related to sources with Z_N charge k , using Monte Carlo simulations. Our results are consistent with the sine formula $\sigma_k/\sigma = \sin k\frac{\pi}{N}/\sin\frac{\pi}{N}$ for the ratio between σ_k and the standard string tension σ . For the $SU(4)$ and $SU(6)$ cases the accuracy is approximately 1% and 2%, respectively. The sine formula is known to emerge in various realizations of supersymmetric $SU(N)$ gauge theories. On the other hand, our results show deviations from Casimir scaling. We also discuss an analogous behavior exhibited by two-dimensional $SU(N) \times SU(N)$ chiral models.

KEYWORDS: confining strings, $SU(N)$ gauge theory, numerical simulations.

Contents

1. Introduction	1
2. k-strings in four-dimensional SU(4) and SU(6) gauge theories	6
3. Strong-coupling expansion in the lattice Hamiltonian approach of SU(N) gauge theories	16
4. Chiral models and lattice gauge theories	19
4.1 Analogies	19
4.2 The two-dimensional SU(N) \times SU(N) chiral models	21
A. Rescaled and effective lattice couplings	23
B. Bulk phase transitions at large N	24
B.1 A first order transition for the SU(6) lattice gauge theory	25
B.2 Just a crossover for the SU(4) lattice gauge theory	26
C. Critical slowing down for the topological modes	27

1. Introduction

Quantum Chromodynamics is a nonabelian gauge theory based on the gauge group SU(3). The mechanisms underlying many of its fundamental properties, such as confinement, chiral symmetry, topological effects and the axial anomaly, are under active investigation; they are being studied by different approaches, including numerical simulations of the theory formulated on the lattice, several models of the vacuum, as well as some recent proposals derived from M-theory and AdS/CFT. Many features of QCD can be better understood by extending the study to SU(N) gauge theories with N larger than three. In particular the large- N limit, which is obtained keeping g^2N fixed (g is the gauge coupling) [1], is of considerable interest from a phenomenological point of view, and is one of our best nonperturbative means of investigating QCD (see e.g. the reviews [2, 3, 4, 5] and references therein). Indeed, this limit is expected to preserve qualitatively most nonperturbative features of QCD.

Four-dimensional non-Abelian gauge theories exhibit confinement, i.e. static sources in the fundamental representation develop a linear potential characterized by

a string tension σ . As pointed out in many studies, it is important to investigate the behavior of the system in the presence of static sources in representations higher than the fundamental one. This may provide useful hints on the mechanism responsible for confinement, helping to identify the most appropriate models of the QCD vacuum and to select among the various confinement hypotheses.

$SU(N)$ gauge theories confine by means of chromoelectric flux tubes carrying charge in the center Z_N of the gauge group. A chromoelectric source of charge k with respect to Z_N is confined by a k -string with string tension σ_k ($\sigma_1 \equiv \sigma$ is the string tension related to the fundamental representation). If $\sigma_k < k\sigma$, then a string with charge k is stable against decay to k strings of unit charge. Charge conjugation implies $\sigma_k = \sigma_{N-k}$. Therefore $SU(3)$ has only one independent string tension determining the large distance behavior of the potential for $k \neq 0$. One must consider larger values of N to search for distinct k -strings. The spectrum of the k -string tensions is then determined by the ratios

$$R(k, N) \equiv \frac{\sigma_k}{\sigma}. \quad (1.1)$$

It has been noted [6] that stable k -strings are related to the totally antisymmetric representations of rank k , and that in various realizations of supersymmetric $SU(N)$ gauge theories $R(k, N)$ satisfies the sine formula $R(k, N) = S(k, N)$ where

$$S(k, N) \equiv \frac{\sin(k\pi/N)}{\sin(\pi/N)}. \quad (1.2)$$

$R(k, N)$ has been computed for the $\mathcal{N} = 2$ supersymmetric $SU(N)$ gauge theory softly broken to $\mathcal{N} = 1$ [9, 10], obtaining Eq. (1.2). The same result has been found also in the context of M-theory, and extended to the case of large breaking of the $\mathcal{N} = 2$ supersymmetric theory [10]. The same formula has been recently rederived [11] using a different setup, i.e. gauge/string duality, suggesting that in the $\mathcal{N} = 1$ supersymmetric gauge theories the sine formula may be quite robust. The interesting question is whether the sine formula holds also in nonsupersymmetric $SU(N)$ gauge theories. The M-theory approach to nonsupersymmetric QCD, although it is still at a rather speculative stage, suggests that this may be so [12, 10]. However, as discussed in Refs. [10, 6], corrections from various sources cannot be excluded, so that this prediction cannot be considered robust.

As pointed out in Ref. [6], it is interesting to compare the k -string tension ratios in different theories. The idea is that such ratios may reveal a universal behavior within a large class of models characterized by $SU(N)$ symmetry, such as $SU(N)$ gauge theories and their supersymmetric extensions. Therefore, according to this universality hypothesis, the k -string tension ratios in four-dimensional $SU(N)$ gauge theories should be given by the sine formula (1.2). This notion of universality for the behavior of the k -string tensions might complement the one conjectured for the type of effective string theory describing confining strings in gauge theories [7, 8].

Another interesting and suggestive hypothesis is that the k -string tension ratio satisfies the so-called Casimir scaling law [13], i.e. $R(k, N) = C(k, N)$ where

$$C(k, N) \equiv \frac{k(N - k)}{N - 1} \quad (1.3)$$

is the ratio between the values of the quadratic Casimir operators in the rank- k anti-symmetric and in the fundamental representations. Casimir scaling is satisfied on the one hand by the small-distance behavior of the potential between two static charges in different representations, as shown by perturbation theory up to two loops [17], and on the other hand by the strong-coupling limit of the lattice Hamiltonian formulation of $SU(N)$ gauge theories [14, 15, 16]. Interest in Casimir scaling was recently revived [18, 19, 20, 21]; it has been triggered by numerical studies of $SU(3)$ lattice gauge theory [22, 23], which indicate that Monte Carlo data for the potential between charges in different representations are consistent with Casimir scaling up to a relatively large distance, $r \approx 1\text{fm}$.

The Casimir scaling law holds exactly in two-dimensional QCD. In higher dimensions no strong arguments exist in favor of a mechanism preserving Casimir scaling from small distance (essentially perturbative, characterized by a Coulombic potential) to large distance (characterized by a string tension for sources carrying Z_N charge); nor across the roughening transition, from strong to weak coupling. We will show explicitly that Casimir scaling does not survive the next-to-leading order calculation of the ratios $R(k, N)$ in the strong-coupling lattice Hamiltonian approach.

It is worth mentioning another simple model for the spectrum of confining strings: if the interaction between fundamental flux tubes were so weak that no bound string states existed, then the spectrum would be given by

$$F(k, N) \equiv \text{Min}[k, N - k]. \quad (1.4)$$

Note that all the above hypotheses considered have the same large- N limit, i.e.

$$S(k, \infty) = C(k, \infty) = F(k, \infty) = k, \quad (1.5)$$

which is the expected result, since no bound states should exist for $N = \infty$. Note also that

$$S(k, N) = k + O(1/N^2). \quad (1.6)$$

In this respect the sine formula is peculiar because there are no a priori reasons for the large- N expansion of the k -string tension ratio to be even in $1/N$.

Of course, it is possible, and even likely given the current state of the theoretical knowledge, that none of the above hypotheses is correct. Nevertheless, we believe that a study able to discard some of them and determining the size of the corresponding corrections would be already important for the understanding of confinement in $SU(N)$ gauge theories.

The issue of the k -strings can be investigated numerically using the lattice formulation of $SU(N)$ gauge theories. Recent numerical results for $R(2, N)$, obtained for $N = 4, 5$ [19, 24], show that $R(2, N) < 2$; thus, $\sigma_2 < 2\sigma$, indicating that flux tubes attract each other, and definitely discarding the hypothesis (1.4) of free strings. The available estimates of $R(2, N)$ are substantially consistent with both the sine and Casimir formulas, thus they do not allow one to exclude any of the two hypotheses. This is also due to the fact that the two predictions for $k = 2$ are numerically close, so that high accuracy is necessary to distinguish them. In particular, the most precise result for the ratio $R(2, 4)$, reported in Ref.[19], lies between the predictions from the sine formula and the Casimir scaling, and is consistent with both within two error bars.

The aim of this paper is to further investigate this issue. We present results from Monte Carlo simulations of the $SU(N)$ lattice gauge theories with $N=4, 6$ using the Wilson formulation. For $N = 4$ two independent k -strings are expected, including the fundamental one. For $N = 6$ there are three. We anticipate here our final results for the k -string tension ratios:

$$R(2, 4) = 1.405 \pm 0.020, \tag{1.7}$$

$$R(2, 6) = 1.72 \pm 0.03, \tag{1.8}$$

$$R(3, 6) = 1.99 \pm 0.07. \tag{1.9}$$

Moreover, we found no evidence for stable string states associated with the symmetric rank-2 representation, in accordance with general arguments.

Figure 1 summarizes our results, comparing our MC results with the above-mentioned hypotheses of spectrum. We claim that $SU(4)$ and $SU(6)$ results show substantial agreement with the sine formula, and therefore with the universality conjecture for the spectrum of the confining strings in asymptotically free theories with $SU(N)$ symmetry. The sine formula (1.2) predicts $S(2, 4) = \sqrt{2} = 1.414\dots$, $S(2, 6) = 1.732\dots$, and $S(3, 6) = 2$. Moreover, the results show deviations from a strict Casimir scaling, whose predictions are $C(2, 4) = 4/3$, $C(2, 6) = 8/5$ and $C(3, 6) = 9/5$.

Considering our results all together, we can state that the sine formula is consistent within an accuracy of approximately 1%. This fact should be relevant for the recent debate on confinement models, such as those discussed in Refs. [18, 19, 20, 21, 25, 26, 27, 28, 29, 30, 31, 32]. Of course, our numerical results cannot prove that the sine formula holds exactly, but they place a very stringent bound on the size of the possible corrections. At the same time, our results appear rather conclusive on the existence of deviations from the Casimir scaling. Casimir scaling may still be considered as a reasonable approximation, since the largest deviation is about 10% for $R(3, 6)$.

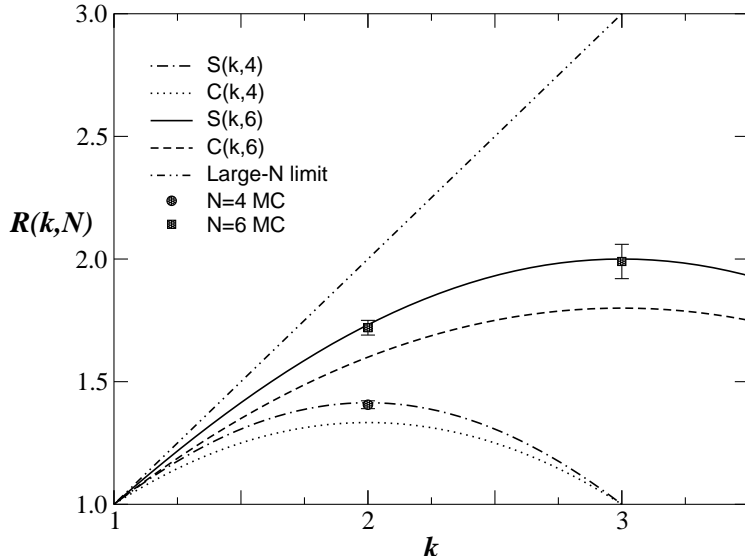


Figure 1: Comparison of the various hypotheses for the k -string ratios with the Monte Carlo results.

Finally, it is interesting to note that the sine formula (1.2) also emerges in the context of the two-dimensional $SU(N) \times SU(N)$ chiral models (see e.g. Ref. [3] as a general reference). d -dimensional chiral models and $2d$ -dimensional lattice gauge theories present interesting analogies. In particular, the relation is exact for $d = 1$, and one can prove that Casimir scaling holds for the masses of the bound states. In analogy with four-dimensional $SU(N)$ gauge theories, in two-dimensional $SU(N) \times SU(N)$ chiral models the Casimir scaling law holds for the small-distance behavior of the correlation functions related to different representations. Moreover, it also holds for the strong-coupling limit of the corresponding lattice Hamiltonians, but it is not satisfied at next-to-leading order for a generic choice of the lattice Hamiltonian, such as the one of Ref. [33]. On the other hand, the exact S-matrix, derived using essentially the Bethe Ansatz [34, 35], shows that bound states exist only for the rank- k antisymmetric representations, and the ratio of their masses satisfies the sine formula.

The paper is organized as follows. In Sec. 2 we present the results of the Monte Carlo simulations of the $SU(4)$ and $SU(6)$ lattice gauge theories. The rest of the paper presents analytical results that help in providing a more detailed picture of the characteristic features of the potential between static charges in higher-rank representations. In Sec. 3 we describe the computation of the strong-coupling expansion in the lattice Hamiltonian approach of $SU(N)$ gauge theories, to the first nontrivial

next-to-leading order. We show explicitly that Casimir scaling is violated by the corrections to the leading order. In Sec. 4 we discuss the analogies between chiral models and lattice gauge theories. The appendices are dedicated to a number of issues related to the Monte Carlo simulations of $SU(N)$ gauge theory at large N , such as the matching of the lattice couplings in the large- N limit, the bulk transition observed at finite bare coupling for N sufficiently large, and the severe form of critical slowing down which characterizes the Monte Carlo dynamics of the topological quantities such as the topological charge, and which appears to follow an exponential law rather than a power law.

Short reports containing essentially our Monte Carlo results for the $SU(6)$ gauge theory, and some preliminary results for $SU(4)$, have already appeared in Refs. [36, 37].

2. k -strings in four-dimensional $SU(4)$ and $SU(6)$ gauge theories

In order to investigate the behavior of the k -string tensions in gauge theories, we performed numerical Monte Carlo simulations of the four-dimensional lattice $SU(4)$ and $SU(6)$ gauge theories using their Wilson formulation

$$S_{\text{gauge}} = -N\beta \sum_{x, \mu > \nu} \text{Tr} [U_\mu(x)U_\nu(x + \mu)U_\mu^\dagger(x + \nu)U_\nu^\dagger(x) + \text{h.c.}]. \quad (2.1)$$

In our simulations we employed the Cabibbo-Marinari algorithm [38] to upgrade $SU(N)$ matrices by updating their $SU(2)$ subgroups (we selected 6 and 15 subgroups respectively for the $SU(4)$ and $SU(6)$ cases). This was done by alternating micro-canonical over-relaxation and heat bath steps, typically in a 4:1 ratio. In the following we consider a sweep as the upgrading of all links of the lattice independently of the algorithm; thus a over-relaxation and heat-bath cycle takes 5 sweeps. In Tables 1 and 2 we present some information on our Monte Carlo runs for the $SU(4)$ and $SU(6)$ cases respectively. We provide the coupling value

$$\gamma \equiv \frac{\beta}{2N^2} \quad (2.2)$$

(this rescaled coupling is more natural for large N , due to the fact that the large- N limit of the lattice theory is obtained keeping γ fixed), the size of the lattices and the number of measurements, reported as the ratio between the number of sweeps N_{sw} and the interval between two measurements N_{m} . Moreover we report the values of the mean field [39, 40] and cactus [41] improved couplings, γ_{mf} and γ_{cactus} respectively, and the value of the lattice spacing in units of the square root of the string tension. As discussed in App. A, these quantities are useful to compare lattice results at

γ	γ_{cactus}	γ_{mf}	lattice	$N_{\text{sw}}/N_{\text{m}}$	$a\sqrt{\sigma}$	$L\sqrt{\sigma}$
0.335	0.24196	0.1862	$12^3 \times 24$	2047k/10	0.2959(14)	3.55
0.338	0.24523	0.1906	$12^3 \times 24$	3858k/20	0.2642(7)	3.17
0.341	0.24850	0.1947	$12^3 \times 24$	4308k/20	0.2368(6)	2.84
0.344	0.25176	0.1987	$12^3 \times 24$	2018k/20	0.2122(8)	2.55
			$16^3 \times 32$	3615k/20	0.2160(8)	3.46

Table 1: Data sets available for SU(4).

γ	γ_{cactus}	γ_{mf}	lattice	$N_{\text{sw}}/N_{\text{m}}$	$a\sqrt{\sigma}$	$L\sqrt{\sigma}$
0.342	0.24234	0.1843	$8^3 \times 16$	213k/10	0.3151(6)	2.52
			$12^3 \times 24$	520k/20	0.3239(8)	3.89
0.344	0.24455	0.1875	$12^3 \times 24$	727k/20	0.2973(5)	3.57
0.348	0.24897	0.1935	$10^3 \times 20$	592k/20	0.2534(6)	2.53
			$12^3 \times 24$	712k/20	0.2535(6)	3.04
0.350	0.25117	0.1963	$12^3 \times 24$	442k/20	0.2380(6)	2.86
0.354	0.25556	0.2017	$12^3 \times 24$	270k/20	0.2103(5)	2.52

Table 2: Data sets available for SU(6).

different values of N . In total, the whole study took about 10 years of CPU on a Pentium III 1Ghz cluster.

The couplings were chosen to lie in the weak-coupling region. This is important because the Wilson lattice formulations of SU(N) gauge theories undergo a first order phase transition for N sufficiently large, as argued using various approaches, such as Monte Carlo simulations [42, 43, 44, 45], mean field calculations [46, 47], reduced models [48]. We found evidence for a first order phase transition in the SU(6) case, for $\gamma_c = 0.3389(4)$. This issue is discussed in App. B, where some additional Monte Carlo results are presented. Therefore, in our simulations we considered γ values larger than γ_c . Moreover, in order to avoid getting trapped in unphysical metastable states, we always used cold configurations as the starting point of our simulations. On the other hand, in the SU(4) case the MC data of the specific heat do not show any evidence for a bulk transition, contrary to some expectations coming from mean field calculations [47] and earlier Monte Carlo simulations [42, 44]. The crossover between the strong- and weak-coupling region is characterized by a pronounced peak of the specific heat at $\gamma \simeq 0.325$ (corresponding to $\beta \simeq 10.4$), similarly to the SU(3) case where the absence of a bulk transition is well established.

We used asymmetric lattices ($L^3 \times T$) with a larger time size, along which the wall-wall correlations of Polyakov loops were measured. For some values of γ we performed simulations for two lattice sizes in order to check for finite size effects. The lattice sizes L were chosen so that $L\sqrt{\sigma} \gtrsim 2.5$, and for most of them $L\sqrt{\sigma} \simeq 3$. This requirement ensures that finite size effects on k -string ratios are negligible, as

can be seen by comparison of the results for different sizes (see also Refs. [49]).

In our simulations we measured also the topological charge Q , by a cooling technique, see e.g. Ref. [50]. A severe form of critical slowing down is observed in this case, which worsens with increasing N . Estimates of the autocorrelation time τ_Q for Q , obtained from a blocking analysis of the data, turns out to be consistent with an exponential increase: $\tau_Q \propto \exp(c\xi_\sigma)$ where $\xi_\sigma \equiv \sigma^{-1/2}$, with $c \approx 1.7$ for SU(4) and $c \approx 2.5$ for SU(6). As a consequence, the run for the largest value of γ we considered for SU(6), i.e. $\gamma = 0.354$, did not correctly sample Q , presumably because it was not sufficiently long ($\approx 300k$ sweeps). This dramatic effect was not observed in the correlators used to determine the k -string tensions, suggesting an approximate decoupling between the topological and nontopological modes. Indeed a blocking analysis did not show significant autocorrelations in measurements taken every 10-20 sweeps. In App. C this issue is discussed in more detail. The critical slowing down shown by the topological quantities represents a severe limitation for numerical studies of the topological properties at large values of N using standard Monte Carlo algorithms. The results related to the topological properties will be reported elsewhere.

The k -string tensions are extracted from the large-time behavior of correlators of strings in the antisymmetric representations, closed through the periodic boundary conditions (see e.g. Refs.[51, 19]):

$$C_r(t) = \sum_{x_1, x_2} \langle \chi_r[P(0; 0)] \chi_r[P(x_1, x_2; t)] \rangle, \quad (2.3)$$

where

$$P(x_1, x_2; t) = \Pi_{x_3} U_3(x_1, x_2, x_3; t). \quad (2.4)$$

$U(\mathbf{x}; t)$ are the usual link variables, and χ_r is the character of the representation r . In particular for the fundamental representation:

$$\chi_f[P] = \text{Tr } P, \quad (2.5)$$

for the antisymmetric representation of rank $k = 2$

$$\chi_{k=2}[P] = \text{Tr } P^2 - (\text{Tr } P)^2, \quad (2.6)$$

and for the antisymmetric representation of rank $k = 3$

$$\chi_{k=3}[P] = 2\text{Tr } P^3 - 3\text{Tr } P^2 \text{Tr } P + (\text{Tr } P)^3. \quad (2.7)$$

These correlators decay exponentially as $\exp(-m_k t)$ where m_k is the mass of the lightest state in the corresponding representation. For a k -loop of size L , the k -string tension is obtained using the relation [51]

$$m_k = \sigma_k L - \frac{\pi}{3L}. \quad (2.8)$$

The last term in Eq. (2.8) is conjectured to be a universal correction, and it is related to the universal critical behavior of the flux excitations described by a free bosonic string [7]. Numerical results for the three- and four-dimensional $SU(N)$ gauge theories with various values of N , see e.g. Refs. [19, 49, 52], and for the three-dimensional Z_2 gauge theory [8] support a universal description of the flux excitations in terms of a free bosonic string. So it is reasonable to assume that this picture, and therefore the relation (2.8), be valid every time that a stable string state propagates, regardless of the gauge group or the representation considered. The comparison of the results obtained for different lattice sizes will give further support to this assumption. Note that Eq. (2.8) is expected to hold for sufficiently large values of L . Ref. [49] argues that a lattice size L satisfying $L\sqrt{\sigma} \gtrsim 3$ should be sufficient to observe a behavior according to Eq. (2.8) for the loop mass. (Although Ref. [49] considered $SU(N)$ gauge theories with $N = 4, 5$, the case $N = 6$ should be equivalent in this respect.)

In order to improve the efficiency of the measurements we used smearing and blocking procedures (see e.g. Refs. [53]) to construct new operators with a better overlap with the lightest string state. The smearing procedure replaces every spatial link on the lattice according to:

$$U_k(x) \mapsto \mathcal{P} \left\{ U_k(x) + \alpha_s \sum_{\pm(j \neq k)} U_j(x) U_k(x + \hat{j}) U_j^\dagger(x + \hat{k}) \right\}, \quad (2.9)$$

where \mathcal{P} indicates the projection onto $SU(N)$ and the sum only runs on spatial directions. The blocking procedure replaces the spatial links with super-links $\mathcal{U}_k(x)$ defined on a lattice with lattice spacing $2a$ (except for the time direction) according to

$$\mathcal{U}_k(x) = \mathcal{P} \left\{ U_k(x) U_k(x + \hat{k}) + \alpha_f \sum_{\pm(j \neq k)} U_j(x) U_k(x + \hat{j}) U_k(x + \hat{j} + \hat{k}) U_j^\dagger(x + 2\hat{k}) \right\}. \quad (2.10)$$

The blocking procedure can then be iterated n times to produce super-links of length $2^n a$. The coefficients α_s and α_f can be adjusted to optimise the efficiency of the procedure. We constructed new super-links using $\alpha_s = \alpha_f = 0.5$, three-smearing, and a few blocking steps, according to the value of L , i.e. one for $L = 10$, two for $L = 8, 12$ and three for $L = 16$. These super-links were used to compute improved Polyakov lines.

We used a standard blocking analysis to check for possible autocorrelations in the wall-wall correlators used to determine the masses. The masses m_k were obtained from fitting the time behaviour of the folded 2-pt correlators:

$$F_{\text{folded}}(t) \equiv \frac{1}{2} (F_k(t) + F_k(N_t - t)) = A(e^{-m_k t} + e^{-m_k(N_t - t)}). \quad (2.11)$$

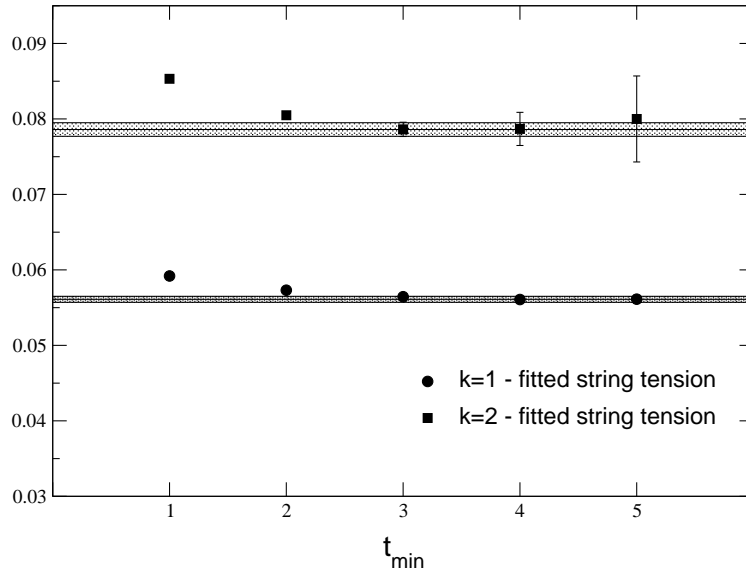


Figure 2: The k -string tensions determined by the fits to the corresponding wall-wall correlations, as functions of the lower bound of the fitrange, t_{\min} , for SU(4) and $\gamma = 0.341$. We also show our final estimates, which are represented by the the continuous lines.

The statistical error on the fitted parameters was computed using a bootstrap procedure.

The choice of the fit range $[t_{\min}, t_{\max}]$ is a delicate issue. In a lattice computation of masses the choice of the fit range is a source of systematic error that is very difficult to control. On the one hand, the data at early times are still contaminated by heavier states. On the other hand, the masses are so large in lattice units that the relative error of data increases rapidly with the distance. A large value of t_{\min} reduces the systematic error due to contamination of heavier states, but leads to an increase of the statistical error. A satisfactory compromise is reached when the two errors are comparable, or, more cautiously, when the systematic error is estimated to be negligible with respect to the statistical one.

The high statistics we collected for the SU(4) lattice gauge theory allowed us to achieve a good control of the systematic error coming from the contamination of heavier states. As an example, we discuss in some detail the analysis of the data obtained for $\gamma = 0.341$, using approximately 2×10^5 measurements. In Fig. 2 we show the results for σ and σ_2 as obtained varying t_{\min} , together with the final estimates that we will quote later. The value of t_{\max} is not critical in this respect, the data reported in the figure have been obtained using $t_{\max} = 8$, but the results are essentially independent of t_{\max} . We observe clearly a dependence on t_{\min} . Our

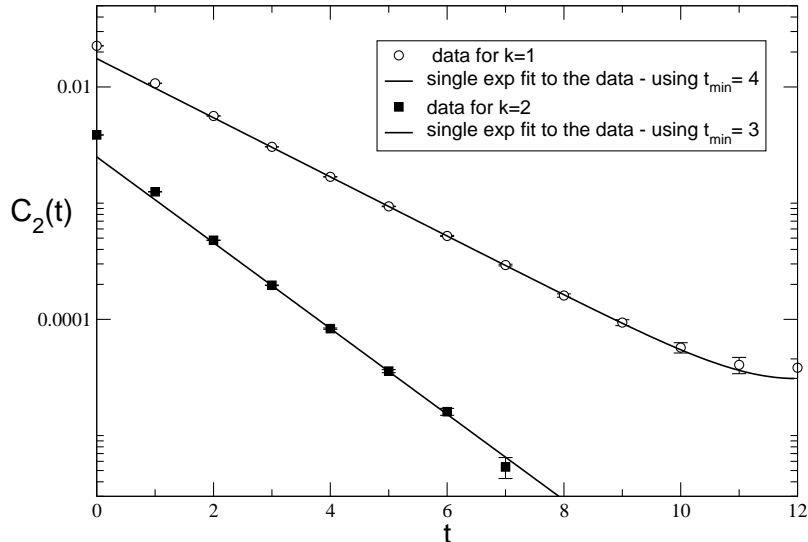


Figure 3: Data for the wall-wall correlations whose large-distance exponential behaviors determine the k -strings, for $SU(4)$ and $\gamma = 0.341$.

estimates are taken when a plateau is reached, i.e. for $t_{\min} = 4$ in the case of σ , and $t_{\min} = 3$ for σ_2 . This should ensure that the systematic error due to heavier states is at most comparable with the statistical one. In Fig. 3 we show the data for the wall-wall correlations corresponding to the fundamental and $k = 2$ antisymmetric representations, and the curves (2.11) with our best estimates of the parameters. Thus we believe that the results and the errors we quote for $SU(4)$ should account for this systematic error.

For the $SU(6)$ lattice gauge theory we could not afford such a clean analysis because of the relatively limited statistics. In this case fits were typically performed in the range $[2 - 4]$ for $\gamma \geq 0.348$, and $[1 - 4]$ for the other values of the coupling. The systematic errors were checked by comparing the outcomes of fits over different time ranges. In practice, we could not use data for distances larger than $t = 5$, which did not allow us to check the dependence on the fit range as satisfactorily as in the $SU(4)$ case. Thus the values of the k -string tensions may be still subject to a systematic error due to the contamination of heavier states. However, we note that the ratios $R(k, N)$ turn out to be more stable with respect to the choice of the fit range (this is already apparent from Fig. 2). We indeed found that the variations of the fit range yield consistent results within the statistical error. So the estimates and the errors that we finally report for the ratios $R(k, N)$ should be reliable also in the $SU(6)$ case.

Results for the k -string tensions obtained in our simulations are reported in Tables 3 and 4 for SU(4) and SU(6), respectively. The relative errors on the ratios $R(2, 4)$, $R(2, 6)$ and $R(3, 6)$ are essentially determined by the uncertainty on σ_2 and σ_3 , since the estimates of σ are in general much more precise. A bootstrap analysis on the data performed directly on the ratios $R(k, N)$, once the fit range has been chosen, usually provides statistical errors that are smaller than the ones we report. However we do not consider them sufficiently reliable, since the systematic error due to the contamination of heavier states is controlled only within the statistical error of the k -string tensions. The ratios $R(2, 4)$, $R(2, 6)$ and $R(3, 6)$ are plotted in Figs. 4, 5, and 6 respectively, versus $a^2\sigma$ to evidenciate possible scaling corrections, which are expected to be $O(a^2)$ apart from logarithms. To facilitate the comparison, in the figures we show the predictions of the sine formula (1.2) and of the Casimir scaling (1.3). Before going into details, it is worthwhile to emphasize some common trends in the results. Data confirm that the finite-size effects on the k -string tension ratios are small for $L\sqrt{\sigma} \gtrsim 2.5$. In all cases the approach to scaling is satisfactory, and the pattern of the scaling corrections turns out to be similar in SU(4) and SU(6).

Let us discuss in more detail the results for the SU(4) gauge theory. Comparing the results obtained at $\gamma = 0.344$ for $L = 12$ and $L = 16$, we see that when $L\sqrt{\sigma} \gtrsim 2.5$ the size effects are small, and within the statistical errors of our data for the k -string ratios. The size effects are instead observable within our statistical errors on σ and σ_2 . The data show a good scaling behavior. Only the results for the smallest value of γ , i.e. $\gamma = 0.335$ apparently show scaling corrections. We extract our final estimate

γ	lattice	$a^2\sigma$	$a^2\sigma_2$	σ_2/σ
0.335	$12^3 \times 24$	0.0876(8)	0.1203(17)	1.374(20)
0.338	$12^3 \times 24$	0.0698(4)	0.0973(12)	1.395(18)
0.341	$12^3 \times 24$	0.0561(3)	0.0786(10)	1.402(17)
0.344	$12^3 \times 24$	0.0450(3)	0.0634(7)	1.407(15)
	$16^3 \times 32$	0.0466(3)	0.0656(9)	1.408(20)

Table 3: k -string tensions for SU(4).

γ	lattice	$a^2\sigma$	$a^2\sigma_2$	$a^2\sigma_3$	σ_2/σ	σ_3/σ
0.342	$8^3 \times 20$	0.0993(4)	0.164(1)	0.190(3)	1.65(2)	1.91(3)
	$12^3 \times 24$	0.1049(5)	0.174(3)	0.201(9)	1.66(3)	1.91(9)
0.344	$12^3 \times 24$	0.0884(3)	0.153(2)	0.173(4)	1.73(2)	1.95(5)
0.348	$10^3 \times 20$	0.0642(3)	0.111(2)	0.134(7)	1.73(3)	2.08(10)
	$12^3 \times 24$	0.0642(3)	0.110(3)	0.132(7)	1.71(4)	2.06(11)
0.350	$12^3 \times 24$	0.0567(3)	0.097(2)	0.110(6)	1.72(3)	1.95(9)
0.354	$12^3 \times 24$	0.0442(2)	0.0766(11)	0.090(3)	1.73(3)	2.04(6)

Table 4: k -string tensions for SU(6).

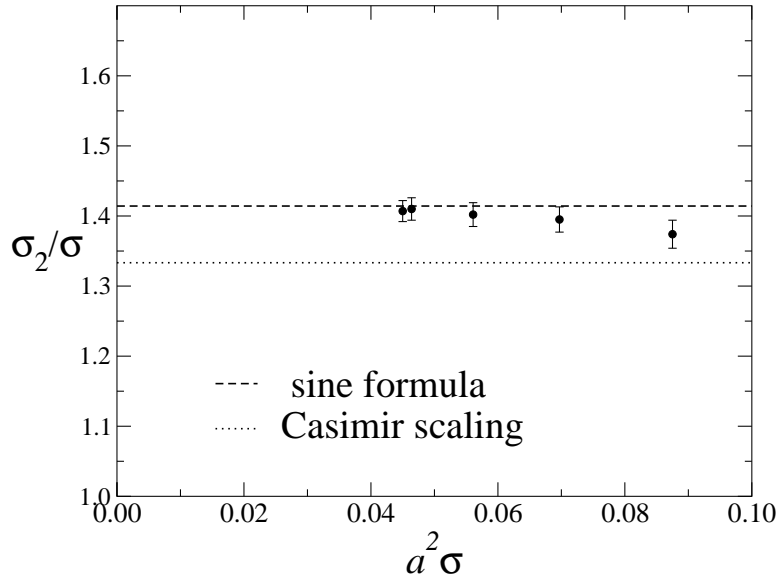


Figure 4: The scaling ratio $R(2, 4)$ as a function of $a^2\sigma$ for $SU(4)$.

for the ratio σ_2/σ from the data at the largest values of γ , i.e. $\gamma = 0.341, 0.344$, and for their corresponding largest lattices. Combining them to obtain the central value and taking the typical error of each single point as estimate of the error, we propose as final estimate $R(2, 4) = 1.405 \pm 0.020$. Of course, this estimate assumes that the scaling corrections are already small and negligible for $a^2\sigma \simeq 0.05$. The data for smaller γ , i.e. $\gamma = 0.335, 0.338$, are used to check this hypothesis. They indicate that the scaling corrections are of the same size as the error we reported above. We will return to this point later. Our result is consistent with the prediction of the sine formula, $S(2, 4) = \sqrt{2} = 1.414\dots$, within an uncertainty of approximately 1%. On the other hand, this result does not support Casimir scaling, whose prediction in this case is $C(2, 4) = 4/3$.

The result obtained in Ref. [19], i.e. $R(2, 4) = 1.357(29)$, is marginally consistent with ours. The comparison improves considering the results $R(2, 4) = 1.377(35)$, obtained in Ref. [19] by discarding the data for the smallest value of β , i.e. $\beta = 10.55$ corresponding to $\gamma = 0.3297\dots$

Let us now consider the results for the $SU(6)$ gauge theory. Comparing the results for the string tension ratios for different lattice sizes at constant γ shows little finite size effects. As in the $SU(4)$ case, finite size effects are observed on the k -string tensions, but they cancel out in the ratios. The ratio $R(2, 6)$ displays good scaling for $\gamma > 0.342$. Given the good scaling behaviour, again we do not attempt to fit the dependence of our result on the lattice spacing a . Our final value for $R(2, 6)$

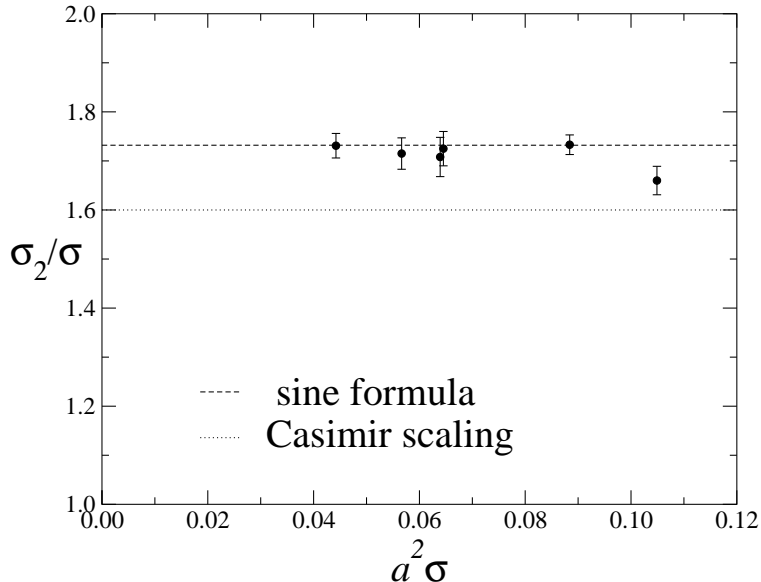


Figure 5: The scaling ratio $R(2,6)$ as a function of $a^2\sigma$ for $SU(6)$.

is obtained averaging the results at $\gamma = 0.348$ and $\gamma = 0.350$, while the error is given by the typical error of each single point. Analogously to the $SU(4)$ case, the data at smaller γ , and in particular the one at $\gamma = 0.344$, are used to check that the scaling corrections are small, and at most comparable with the error we report. Given the poor sampling of the topological charge in the run at $\gamma = 0.354$, we do not include this value of γ in the final estimate of the string tension ratio. Similar comments apply to the $R(3,6)$ ratio. We finally note that the results for $R(k,6)$ at $\gamma = 0.354$ are in agreement with those obtained at smaller values of γ , for which Q was sampled correctly, lending further support to the previously mentioned large decoupling of the modes determining the string tensions and the topological ones. As anticipated in the introduction, our final estimates are $R(2,6) = 1.72 \pm 0.03$ and $R(3,6) = 1.99 \pm 0.07$. They are both consistent with the predictions of the sine formula (1.2), which are $S(2,6) = 1.732\dots$ and $S(3,6) = 2$, respectively, within an uncertainty of approximately 2% for $k = 2$ and 4% for $k = 3$. On the other hand, they do not support Casimir scaling; the predictions in this case are $C(2,6) = 8/5$ and $C(3,6) = 9/5$.

We have also explored correlators in the symmetric rank-2 representation, whose character is given by

$$\chi_{k=2,\text{symm}}[P] = \text{Tr } P^2 + (\text{Tr } P)^2, \quad (2.12)$$

finding no evidence for new stable string states for both $SU(4)$ and $SU(6)$ cases. The masses extracted in the symmetric channel were consistent with $m_{\text{symm}} \geq 2m_f$, as

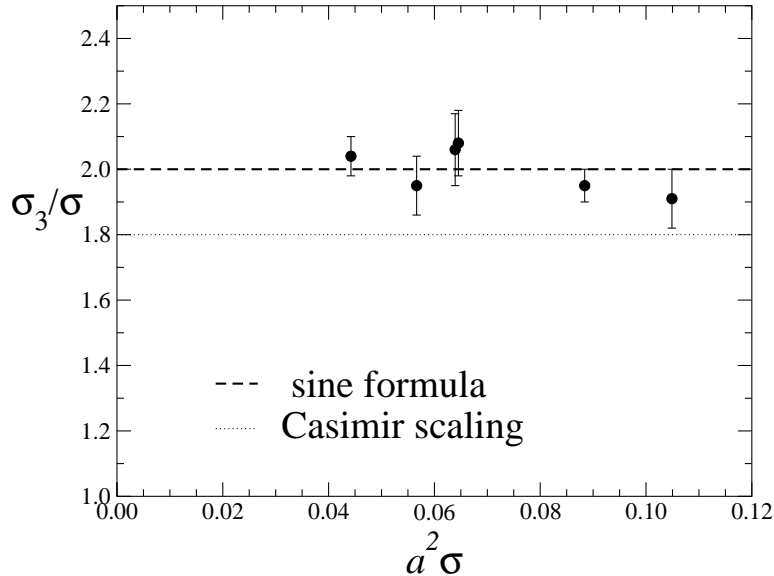


Figure 6: The scaling ratio $R(3,6)$ as a function of $a^2\sigma$ for $SU(6)$.

expected because the symmetric string should indeed decay into two fundamental strings. In this case, Eq. (2.8) should not apply and we did not try to extract a string tension.

In conclusion, our results turn out to be consistent with the sine formula, and show that there are sizeable corrections to the Casimir scaling prediction. In order to further check the robustness of our statement concerning the deviation from the Casimir formula, we have analyzed our data using also fits which allow explicitly for scaling corrections. As suggested in Ref. [19], one may fit the data to the linear behavior $A + B\sigma$. For this purpose one must consider all data, including the ones for the smallest values of γ , since they are the only ones showing apparent scaling violations. In the $SU(4)$ case we find $R(2,4) = 1.450(32)$ with $\chi^2 \simeq 0.2$. In the $SU(6)$ case the results are $R(2,6) = 1.76(4)$ ($\chi^2 \simeq 2.6$), $R(3,6) = 2.13(11)$ ($\chi^2 \simeq 1.4$) and $R(2,6) = 1.77(6)$ ($\chi^2 \simeq 2.7$), $R(3,6) = 2.16(19)$ ($\chi^2 \simeq 1.3$) respectively with and without the point at the largest value of γ , i.e. $\gamma = 0.354$. Therefore, if one wants to be more cautious in treating the systematic error due to scaling corrections, one may take into account the difference between the linear fits and the nonextrapolated data, yielding

$$R(2,4) = 1.405 \pm 0.020 \begin{matrix} +0.045 \\ -0.000 \end{matrix}, \quad (2.13)$$

$$R(2,6) = 1.72 \pm 0.03 \begin{matrix} +0.05 \\ -0.00 \end{matrix}, \quad (2.14)$$

$$R(3,6) = 1.99 \pm 0.07 \begin{matrix} +0.17 \\ -0.00 \end{matrix}, \quad (2.15)$$

which cover all the results obtained above. These conservative estimates are still not consistent with the Casimir formula. Thus, our conclusions are fully justified even by this overly cautious analysis. One should note that corrections to Casimir scaling are to be expected as discussed in the previous section (see also Sec. 3). The implications of these results for models of the Yang-Mills vacuum deserve further investigation.

One may write down a general expression for $R(k, N)$ taking into account the following constraints: $R(1, N) = 1$ by definition, $R(k, N) = R(N - k, N)$ by charge conjugation, and $R(k, \infty) = k$ which is the expected large- N limit. A general expression satisfying these conditions can be written as

$$G(k, N) = \frac{U(k, N)}{U(1, N)}, \quad (2.16)$$

where

$$U(k, N) = \sin \frac{k\pi}{N} \left[1 + \sum_{i=1} c_i(N) \left(\sin \frac{k\pi}{N} \right)^i \right] \quad (2.17)$$

and c_i are coefficients which may depend on N , but in such a way as not to spoil the large- N limit, i.e. $c_i(N)/N^i = O(1/N)$. Our results show that, if the sine formula is not exactly satisfied, the corrections must be small, thus $c_i \ll 1$. In order to better quantify this statement, one may keep only the first term in the sum of Eq. (2.17) and find a bound on c_1 (assuming it constant). Our Monte Carlo results provide the bound $|c_1| \lesssim 0.05$. We think that the accuracy of the sine formula in predicting the σ_k/σ ratio should trigger further fundamental theoretical investigations.

3. Strong-coupling expansion in the lattice Hamiltonian approach of $SU(N)$ gauge theories

The strong-coupling expansion in the lattice Hamiltonian formulation of the theory is an analytical approach that can be used to investigate Casimir scaling and its corrections.

The lattice Hamiltonian of a D -dimensional $SU(N)$ gauge theory is defined in terms of link operators in the fundamental representation $\hat{U}_\mu(x)$. Following Ref. [14], we consider the Hamiltonian

$$H_{\text{gauge}} = \frac{g^2}{2a} \left\{ \sum_l \hat{E}^2(l) - \frac{2}{g^4} \sum_p \text{Tr} \left[\hat{U}(p) + h.c. \right] \right\}, \quad (3.1)$$

where $\hat{E}^2(l) \equiv \sum_{a=1}^{N^2-1} \hat{E}^a(l) \hat{E}^a(l)$ is the quadratic Casimir operator of $SU(N)$ associated with the link l of a $(D-1)$ -dimensional cubic lattice, and $\hat{U}(p)$ is the product of link operators on the boundary of a plaquette p . The $SU(N)$ gauge theory is realized in the continuum limit $g \rightarrow 0$. The lattice Hamiltonian formulation is not unique,

and therefore the corresponding strong-coupling expansion in powers of $1/g$ should be considered as a suggestive investigation method, but it is difficult to extract reliable quantitative information from it.

In the perturbative strong-coupling approach in which $g \rightarrow \infty$, one works in the space of states $\prod_x |U\rangle$ diagonal in \hat{U} :

$$\hat{U}_r^{ab}|U\rangle = U_r^{ab}|U\rangle, \quad (3.2)$$

$$[\hat{E}^a, \hat{U}_r] = -\frac{1}{2}\lambda_r^a \hat{U}_r, \quad (3.3)$$

where r indicates the generic representation and λ_r^a the corresponding generators. In the strong-coupling limit $g \rightarrow \infty$, the vacuum $|0\rangle$ is the lowest eigenstate of

$$H_0 \equiv A \sum_l \hat{E}^2(l), \quad (3.4)$$

where $A = g^2/2a$, thus it satisfies $\hat{E}^2|0\rangle = 0$. In order to compute the k -string tensions, we must consider the force law between widely separated quarks in the strongly coupled limit. The potential energy is defined as the lowest energy compatible with the presence of a quark q at the origin and an antiquark \bar{q} at site s . The minimum-energy gauge-invariant state is obtained by exciting the shortest path of links connecting the $q\bar{q}$ pair. Let us take the $q\bar{q}$ pair along a side of the cubic lattice, thus the least number of excited links is $l = s$. In the strong-coupling limit $g \rightarrow \infty$ it can be written as the product of l link operators joining the origin to the site s :

$$|r, l\rangle = d_r^{-1/2} \hat{U}_r(1) \hat{U}_r(2) \dots \hat{U}_r(s) |0\rangle, \quad (3.5)$$

where r is the representation of $SU(N)$ considered and d_r its dimension. The inner product $\langle | \rangle$ is defined using the invariant integration over the group:

$$\int dg U_r^{ab} \bar{U}_{r'}^{a'b'} = d_r^{-1} \delta_{rr'} \delta_{aa'} \delta_{bb'}. \quad (3.6)$$

The energy corresponding to the state $|r, l\rangle$ is given by the matrix element $\langle r, l | H_0 | r, l \rangle$. As already mentioned, the leading order of the energy is proportional to $C_r = \frac{1}{4} \lambda_r^a \lambda_r^a$, the value of the quadratic Casimir operator in the representation r , i.e.

$$\langle r, l | H_0 | r, l \rangle = A l C_r. \quad (3.7)$$

Higher order corrections can be computed by systematic application of perturbation theory, where the perturbation interaction H_I is given by the second term of the Hamiltonian (3.1). The perturbation H_I corrects the energy of these states and of the vacuum to $O(1/g^8)$, i.e. to second order in perturbation theory. These corrections are obtained by computing

$$\langle r, l | H_I \frac{1}{E - H_0} H_I | r, l \rangle \quad (3.8)$$

and subtracting the corresponding second order contribution to the vacuum energy

$$\langle 0 | H_I \frac{1}{-H_0} H_I | 0 \rangle. \quad (3.9)$$

For the k -string tension associated with the rank- k antisymmetric representation $(1^k; 0)$ (where 1^k indicates one column with k squares in the corresponding Young tableau) we obtain

$$\sigma_k = A C_{(1^k; 0)} \left[1 + \frac{D-2}{(g^2 N)^4} e_4(k, N) + O\left(\frac{1}{(g^2 N)^6}\right) \right], \quad (3.10)$$

where $C_{(1^k; 0)}$ is the value of the quadratic Casimir operator for the representation $(1^k; 0)$, and

$$e_4(k, N) = \frac{8N^4}{C_{(1^k; 0)}} \left[\frac{1}{2C_{(1; 0)}} + \sum_{i=1}^4 \frac{1}{C_{(1^k; 0)} - 3C_{(1; 0)} - C_{r_i}} \frac{d_{r_i}}{Nd_{(1^k; 0)}} \right]. \quad (3.11)$$

The sum extends over the four representations r_i obtained by composing the rank- k antisymmetric representation $(1^k; 0)$ with the fundamental $(1; 0)$ and antifundamental $(0; 1)$ representations, i.e. $(1^{k+1}; 0)$, $(2, 1^{k-1}; 0)$ and $(1^{k-1}; 0)$, $(1^k; 1)$ respectively. For notation see e.g. Ref. [4]. The corresponding dimensions d_{r_i} and Casimir values C_{r_i} are

$$d_{(1^k; 0)} = \binom{N}{k}, \quad (3.12)$$

$$C_{(1^k; 0)} = \frac{k(N+1)(N-k)}{2N}, \quad (3.13)$$

$$d_{(2, 1^{k-1}; 0)} = k \binom{N+1}{k+1}, \quad (3.14)$$

$$C_{(2, 1^{k-1}; 0)} = \frac{(k+1)[N^2 - N(k-2) - k - 1]}{2N}, \quad (3.15)$$

$$d_{(1^k; 1)} = d_{(2, 1^{N-k-1}; 0)}, \quad (3.16)$$

$$C_{(1^k; 1)} = C_{(2, 1^{N-k-1}; 0)}. \quad (3.17)$$

Notice that in the above expressions $(1^0; 0) \equiv (0; 0)$, i.e. the singlet representation. For $k = 1$, i.e. the fundamental string tension, the expression (3.10) reproduces the result reported in Ref. [54], i.e.

$$\sigma = A \frac{N^2 - 1}{2N} \left[1 - \frac{D-2}{(g^2 N)^4} \frac{16N^6(3N^2 - 5)}{(N^2 - 1)^2(2N^2 - 1)(4N^2 - 9)} + \dots \right]. \quad (3.18)$$

One can easily see that $e_4(k, N)$ satisfies the relation $e_4(k, N) = e_4(N - k, N)$. It has the expected limit for $N \rightarrow \infty$, indeed the term coming from the subtraction of the

vacuum contribution, which is the first one in Eq. (3.11), cancels the leading power in N , and the expression goes to a constant for $N \rightarrow \infty$.

For the k -string tension ratio we obtain

$$\frac{\sigma_k}{\sigma} = \frac{k(N-k)}{N-1} \left\{ 1 + \frac{D-2}{(g^2 N)^4} [e_4(k, N) - e_4(1, N)] + O\left(\frac{1}{(g^2 N)^6}\right) \right\}. \quad (3.19)$$

Explicitly for $k = 2$,

$$\begin{aligned} e_4(2, N) - e_4(1, N) &= \\ &= \frac{4N^3(N-3)(12N^6 + 14N^5 - 46N^4 - 47N^3 + 61N^2 + 34N - 24)}{(N-2)(2N-3)(2N+3)(N^2-1)^2(2N^2-1)(2N^2+N-4)} \\ &= \frac{6}{N} - \frac{2}{N^2} + O\left(\frac{1}{N^3}\right). \end{aligned} \quad (3.20)$$

Note that the correction to the leading order Casimir scaling is $O(1/N)$.

This result provides an explicit example of corrections to the Casimir scaling prediction: while the leading order strong coupling calculation yields Casimir scaling, $O(1/N)$ corrections arise at the next-to-leading order. This fact holds for both $D = 4$ and $D = 3$.

4. Chiral models and lattice gauge theories

In this section we discuss the analogies existing between $2d$ -dimensional $SU(N)$ gauge theories and d -dimensional $SU(N) \times SU(N)$ chiral models. In particular, we compare the spectrum of the k -strings in $SU(N)$ gauge theories with the known spectrum of the bound states in chiral models.

4.1 Analogies

Unitary matrix models defined on a lattice can be divided into two major groups, according to the geometric and algebraic properties of the dynamical variables: when the fields are defined in association with lattice sites, and the symmetry group is global, i.e., a single $SU(N)_L \times SU(N)_R$ transformation is applied to all fields, we are considering a spin model (principal chiral model); in turn, when the dynamical variables are defined on the links of the lattice and the symmetry is local, we are dealing with a gauge model (lattice gauge theory). An analogy between d -dimensional chiral models and $2d$ -dimensional gauge theories can be found according to the following correspondence table [55, 3]:

spin	gauge
site, link	link, plaquette
loop	surface
length	area
mass M	string tension σ
two-point correlation	Wilson loop

To this correspondence table, one may also add: the spectrum of the bound states on the side of the chiral models and the spectrum of confining strings for $SU(N)$ gauge theories, i.e.

spin	gauge
bound state mass M_k	k -string tension σ_k

While the above correspondence in arbitrary dimensions is by no means rigorous, there is some evidence supporting the analogy.

Let us consider the following lattice formulation of d -dimensional $SU(N) \times SU(N)$ principal chiral models

$$S_{\text{chiral}} = -2N\beta \sum_{x,\mu} \text{ReTr} [U(x)U^\dagger(x + \mu)] \quad (4.1)$$

(where $\beta = 1/NT$, $U_x \in SU(N)$ and $\mu = 1, \dots, d$); for $SU(N)$ gauge theories in $2d$ dimensions we consider the Wilson lattice formulation (2.1).

In the case $d = 1$ one can prove an identity between the partition function (and appropriate correlation functions) of the two-dimensional lattice gauge theory and the corresponding quantities of the one-dimensional principal chiral model (see e.g. Ref. [4]). Both theories are exactly solvable and the correspondence can be explicitly shown. In particular, using the results of Ref. [56], one may easily show that the Casimir formula holds for the spectrum. Thus

$$\frac{M_k}{M} = \frac{k(N - k)}{N - 1} \quad (4.2)$$

holds for the one-dimensional $SU(N) \times SU(N)$ chiral models, and

$$\frac{\sigma_k}{\sigma} = \frac{k(N - k)}{N - 1} \quad (4.3)$$

for two-dimensional $SU(N)$ gauge theories.

Although for higher dimensions the correspondence does not strictly hold, we still have some analogies:

(i) The two-dimensional chiral model and the four-dimensional non-abelian gauge theory share the property of asymptotic freedom and dynamical generation of a mass scale. In both models these properties are absent in the Abelian case (XY model and $U(1)$ gauge theory respectively).

(ii) The classical equations of motion describing the dynamics of the spin variables in the two-dimensional chiral model and the Wilson loops in the four-dimensional nonabelian gauge theory are similar (see e.g. Ref. [3]). It turns out that the gauge fields are chiral fields on the loop space. This analogy persists at the quantum level as well, since the classical equations of motion dictate relations among correlation functions in the corresponding quantum theory.

(iii) Exploiting asymptotic freedom, one can use perturbation theory to determine the short-distance behavior of the potential of two heavy quarks in four-dimensional $SU(N)$ gauge theories and of the two-point correlation function in two-dimensional $SU(N) \times SU(N)$ chiral models. Both show Casimir scaling. In the four-dimensional $SU(N)$ gauge theory the force $F_r(x)$ between two heavy quarks in the representation r is proportional to C_r up to two loops [17]. Resumming the leading logarithms using standard renormalization-group arguments, the short-distance behavior of the force $F_r(x)$ is:

$$F_r(x) = -C_r \frac{\alpha_r(1/x)}{x^2},$$

$$\alpha_r(1/x) = \frac{1}{b_0 L(x)} \left[1 - b_1 \frac{\ln L(x)}{L(x)} + O\left(\frac{(\ln L)^2}{L^2}\right) \right],$$

where $L(x) = -\ln x \Lambda_x$ and Λ_x is a mass scale (the so-called Λ -parameter associated with the above definition of running couplings $\alpha_r(x)$; b_0 and b_1 are the first two universal coefficients of the perturbative expansion of the β -function $\beta(\alpha) = -x \partial \alpha_r / \partial x$. b_0 , b_1 and Λ_x are independent of C_r . A dependence on C_r of the $O((\ln L)^2/L^2)$ term in $\alpha_r(1/x)$ is not excluded. Its computation requires a three-loop calculation of the potential. As we shall see in Sec. 4.2, Casimir scaling emerges also in the short-distance behavior of two-point functions in chiral models.

(iv) Another analogy concerns the large- N limit, which in both cases is given by a sum of planar graphs. In this limit particles in chiral theories become free, indeed the known S-matrix [34, 35] becomes trivial. On the other hand, it is conjectured that the large- N limit of gauge theories is a free string theory, see e.g. [3], although its nature is still not clear.

(v) Their strong-coupling expansions look similar, provided that point-like excitations of chiral fields are substituted by closed flux lines for the gauge fields.

(vi) Approximate real-space renormalization recursion relations obtained by Migdal [57] are identical for d -dimensional chiral models and $2d$ -dimensional gauge models.

4.2 The two-dimensional $SU(N) \times SU(N)$ chiral models

The two-dimensional $SU(N) \times SU(N)$ principal chiral models are asymptotically free matrix-valued field theories defined by the action

$$S = \frac{1}{T} \int d^2x \text{Tr} \partial_\mu U(x) \partial_\mu U^\dagger(x). \quad (4.4)$$

where $U(x) \in SU(N)$.

Using the existence of an infinite number of conservation laws and Bethe-Ansatz methods, the on-shell solution of the $SU(N) \times SU(N)$ chiral models has been proposed

in terms of a factorized S-matrix [34, 35]. The analysis of the corresponding bound states leads to the mass spectrum

$$M_k = M \frac{\sin(k\pi/N)}{\sin(\pi/N)}, \quad 1 \leq k \leq N-1, \quad (4.5)$$

where M_k is the mass of the k -particle bound state transforming as a totally antisymmetric tensor of rank k . $M \equiv M_1$ is the mass of the fundamental state determining the Euclidean long-distance exponential behavior of the two-point Green's function

$$G(x) = \frac{1}{N} \langle \text{Tr } U(0)U(x)^\dagger \rangle. \quad (4.6)$$

No bound states exist for other representations. Correlation functions associated with the generic representation r can be defined by

$$G_r(x) = \frac{1}{d_r} \langle \chi_r [U(0)U(x)^\dagger] \rangle, \quad (4.7)$$

where d_r and χ_r are respectively the dimension and the character of the representation r . The structure of the S-matrix implies that stable bound states propagate only in the totally antisymmetric representations with masses given by Eq. (4.5). Note that, according to the correspondence discussed in Sec. 4.1, the correlation functions $G_r(x)$ play the role of the r -representation Wilson loops for $SU(N)$ gauge theories. The mass spectrum (4.5) has been verified numerically at $N = 6$ by Monte Carlo simulations [58, 59].

As in $SU(N)$ gauge theories, the large- N limit of these models is formally represented by a sum over planar graphs. The S -matrix has a convergent expansion in powers of $1/N$, and becomes trivial, i.e., the S -matrix of free particles, in the large- N limit. Note also that, as in the case of $SU(N)$ gauge theories, no a priori reasons exist for the large- N expansion of the k -state mass ratios (4.5) to be even in $1/N$.

Asymptotic freedom allows us to determine the small-distance behavior of the correlation functions in perturbation theory. In two-dimensional $SU(N) \times SU(N)$ chiral models, the logarithm of the two-point function $G_r(x)$ is the analog of the potential of two separated quarks in the representation r . The small-distance behavior of $\ln G_r(x)$ satisfies Casimir scaling, similarly to what happens for the potentials in four-dimensional $SU(N)$ gauge theories. Extending the results of Ref. [60] pertaining to the fundamental two-point function, in the \overline{MS} renormalization scheme associated with the x space we find

$$\begin{aligned} \ln G_r(x) = & -C_r t \left\{ \ln(\mu x) + \frac{N}{8} t \ln(\mu x)^2 \right. \\ & \left. + t^2 \left[\frac{N^2}{256} (3 - 2\zeta(3)) + \frac{3N^2}{128} \ln(\mu x) + \frac{N^2}{64} \ln(\mu x)^2 + \frac{N^2}{48} \ln(\mu x)^3 \right] + O(t^3) \right\}, \end{aligned} \quad (4.8)$$

where C_r is the Casimir value of the representation r . As in four-dimensional $SU(N)$ gauge theories, one may define a running coupling t_x from the relation

$$-\frac{\partial \ln G_r(x)}{\partial x} = C_r \frac{t_x}{x}. \quad (4.9)$$

Standard renormalization-group arguments allow one to resum the leading logarithms, yielding

$$t_x = \frac{1}{b_0 L(x)} \left[1 - \frac{b_1 \ln L(x)}{L(x)} + O\left(\frac{(\ln L)^2}{L^2}\right) \right]. \quad (4.10)$$

As before, $L(x) = -\ln x \Lambda_x$ and Λ_x is a mass scale; $b_0 = N/(8\pi)$, $b_1 = N^2/(128\pi^2)$ are the first two coefficients of the β -function $\beta(t_x) = -x \partial t_x / \partial x = -b_0 t_x^2 - b_1 t_x^3 + O(t_x^4)$. We also mention that at the next order of perturbation theory, i.e. $O(t^4)$ in Eq. (4.8), there are three-loop diagrams whose group factor would violate Casimir scaling. Thus, barring particular cancellations, Casimir scaling should not be satisfied by the $O((\ln L)^2/L^3)$ term of Eq. (4.10). The same observation applies to four-dimensional $SU(N)$ gauge theories.

Finally, again similarly to QCD, one may easily check that, using the lattice Hamiltonian approach of Ref. [33], Casimir scaling is recovered in the strong-coupling limit; it is violated by higher order corrections.

The analogy with chiral models highlights some general trends: Casimir scaling is exact in $d = 1$, as it is in the case of $SU(N)$ Yang Mills theories in $d = 2$; for $d = 2$, both perturbation theory and strong coupling yield Casimir scaling to lowest order. However next-to-leading order calculations explicitly show corrections to such behavior. This fact is consistent with the picture that emerges for $d = 4$ $SU(N)$ gauge theories from our Monte Carlo simulations.

Acknowledgments

We thank M. Campostrini, K. Konishi, S. Lelli, B. Lucini, M. Maggiore, A. Pelissetto, V. Shevchenko, and M. Teper for useful and interesting discussions. LDD enjoyed the warm hospitality of the Theoretical Physics Department in Oxford, where some of the above discussions took place. H. P. would like to thank the Theory Group in Pisa for their hospitality during various stages of this work. We thank Maurizio Davini for setting up the cluster that ran the simulations and for his indispensable technical support.

A. Rescaled and effective lattice couplings

In order to compare Monte Carlo results for various values of N , it is useful to introduce the rescaled coupling

$$\gamma \equiv \frac{1}{g_0^2 N} = \frac{\beta}{2N^2} \quad (A.1)$$

which is kept fixed in the large- N limit of the lattice theory, see e.g. Refs. [2, 4]. As already noted in Refs. [61, 49], the correspondence of the bare couplings for models with different values of N (defined keeping physical quantities such as the string tension fixed) becomes more accurate if one uses the mean field improved coupling g_{mf} proposed in Refs. [39, 40] and obtained by dividing the lattice coupling g_0^2 by the average value of the plaquette, i.e.

$$g_{\text{mf}}^2 = \frac{g_0^2}{\langle \frac{1}{N} \text{Tr} U_{\mu\nu}(x) \rangle}. \quad (\text{A.2})$$

Here we also consider the effective coupling g_{cactus}^2 obtained within an all-order resummation of cactus-type diagrams in perturbation theory [41], and defined by

$$g_{\text{cactus}}^2 = \frac{g_0^2}{w(g_0)}. \quad (\text{A.3})$$

The function $w(g_0)$ can be extracted by an appropriate algebraic equation that can be easily solved numerically:

$$u e^{-u(N-1)/(2N)} \left[\frac{N-1}{N} L_{N-1}^1(u) + 2L_{N-2}^2(u) \right] = \frac{g_0^2 (N^2-1)}{4}, \quad (\text{A.4})$$

$$u(g_0) \equiv \frac{g_0^2}{4(1-w(g_0))},$$

where L_N^M are the Laguerre polynomials. Data for $N = 3, 4, 6$ are shown in Fig. 7 (the data for $N = 3$ and some of those for $N = 4$ have been taken from Ref. [49]): we plot $1/\gamma = Ng_0^2$, $1/\gamma_{\text{mf}} = Ng_{\text{mf}}^2$ and $1/\gamma_{\text{cactus}} = Ng_{\text{cactus}}^2$ versus $a\sigma^{1/2}$, where σ is the string tension. The gray points, corresponding to the mean field improved coupling, fall approximately on a single curve. A similar behaviour is observed for the cactus improved coupling (black points), while the data corresponding to the bare coupling (white points) show a wider spread as N is varied. We conclude that both the improved couplings provide an efficient tool to match theories at different values of N . In this respect, the mean field improved coupling performs slightly better, but the advantage of the cactus definition is that it is determined from Eq. (A.4), without requiring any simulation.

B. Bulk phase transitions at large N

For sufficiently large values of N and in particular in the large- N limit, the Wilson lattice formulation of $\text{SU}(N)$ gauge theories presents a first order phase transition. This has been argued using various approaches, such as Monte Carlo simulations [42, 43, 44, 45], mean field calculations [46, 47], reduced models [48]. In the following we present evidence for a first order transition at a finite bare coupling in the case of the $\text{SU}(6)$ lattice gauge theory. On the other hand, in the $\text{SU}(4)$ case no evidence of a bulk phase transition is found.

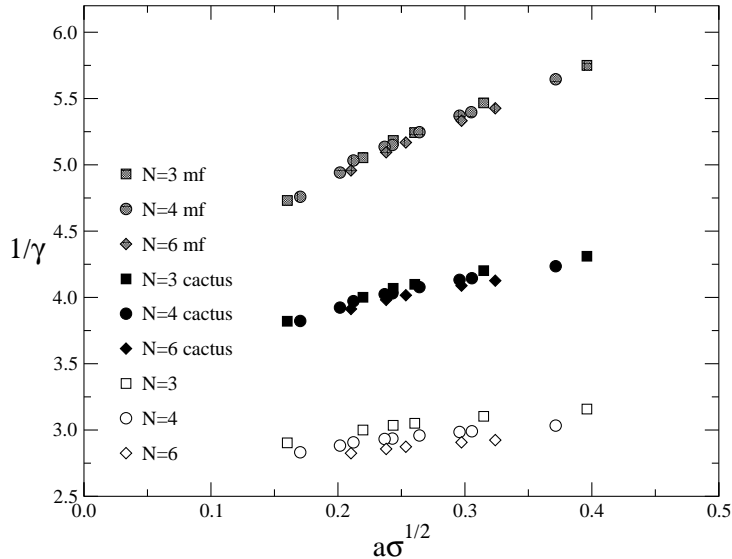


Figure 7: $1/\gamma$, $1/\gamma_{\text{mf}}$ and $1/\gamma_{\text{cactus}}$ versus $a\sigma^{1/2}$ for SU(3), SU(4), and SU(6) lattice gauge theories.

B.1 A first order transition for the SU(6) lattice gauge theory

In the case $N = 6$, we performed simulations starting from hot and cold configurations. Fig. 8 reports data for the energy density E (normalized to one for $\gamma = 0$) obtained performing two simulations on a 8^4 lattice, one starting from a hot configuration and the other from a cold configuration. More precisely, in the first case we started from a hot configuration, and performed simulations starting from $\gamma = 0.334$, increasing the value of γ every 2000 heat bath updatings by 0.001. The data reported in the figure are the values of the energy obtained averaging over the second 1000 updatings for each γ value. The data concerning the simulation starting from a cold configuration were obtained similarly, i.e. starting from $\gamma = 0.344$ and decreasing its value by 0.001 every 2000 upgradings. Fig. 8 shows clearly the presence of hysteresis, from which one may estimate $\gamma_c \approx 0.339$. Note that the latent heat is relatively large indicating that the first order transition is rather strong. Another estimate of γ_c can be obtained from the so-called mixed-phase method. One starts from a configuration that is half cold and half hot, and see which phase wins as γ is varied. An estimate of γ_c is obtained from the boundary values of γ for which the change of final phase occurs. The two phases are easily recognized by their value of the energy: as shown in Fig. 8, $E_{\text{hot}} \simeq 0.57$ and $E_{\text{cold}} \simeq 0.47$ at γ_c . We obtained $\gamma_c \approx 0.3393$, $\gamma_c \approx 0.3390$ and $\gamma_c \approx 0.3389$ respectively from simulations on 8^4 , 10^4 and 12^4 lattices. As a final estimate we consider $\gamma_c = 0.3389(4)$. For comparison, we mention the earlier

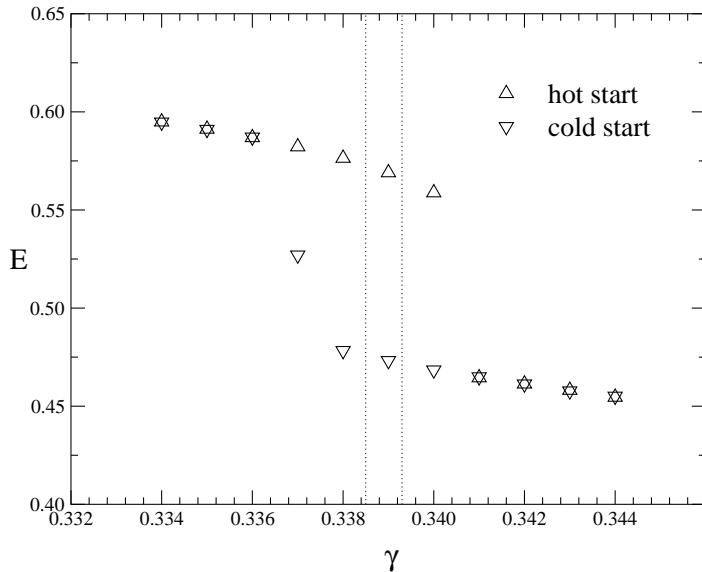


Figure 8: Energy density versus γ obtained as explained in the text. The two vertical lines show the estimate of γ_c obtained by the mixed-phase method.

estimate $\gamma_c = 0.333(14)$ [43].

B.2 Just a crossover for the SU(4) lattice gauge theory

In the case of the SU(4) lattice gauge theory, no evidence for a bulk transition is observed. In particular, the specific heat does not appear to diverge with increasing lattice size. In Fig. 9 we plot data for the specific heat

$$C_H = -\beta^2 \frac{d}{d\beta} \left(1 - \frac{1}{N} \langle \text{Tr } U_{\mu\nu}(x) \rangle \right) \quad (\text{B.1})$$

for various lattice sizes, i.e. 6^4 , 8^4 and 12^4 . The data were obtained from runs with typical statistics of $3\text{-}5 \times 10^4$ sweeps. They show a rather pronounced peak around $\gamma \simeq 0.325$ (corresponding to $\beta = 10.4$), but they appear to converge for increasing lattice size. We recall that, in the case of a first order phase transition, the finite-size scaling behavior of the peak value of the specific heat should diverge as [62]

$$C_{H,\text{peak}} \sim L^d, \quad (\text{B.2})$$

thus $C_{H,\text{peak}} \sim L^4$ in our case. The data of Fig. 9 are clearly inconsistent with such a behavior. These results indicate that the Wilson formulation of the SU(4) lattice gauge theory does not undergo a first-order phase transition, but rather they suggest that, as in the SU(3) case, it exhibits a crossover between the strong and weak coupling regime, characterized by a rather pronounced peak of the specific heat.

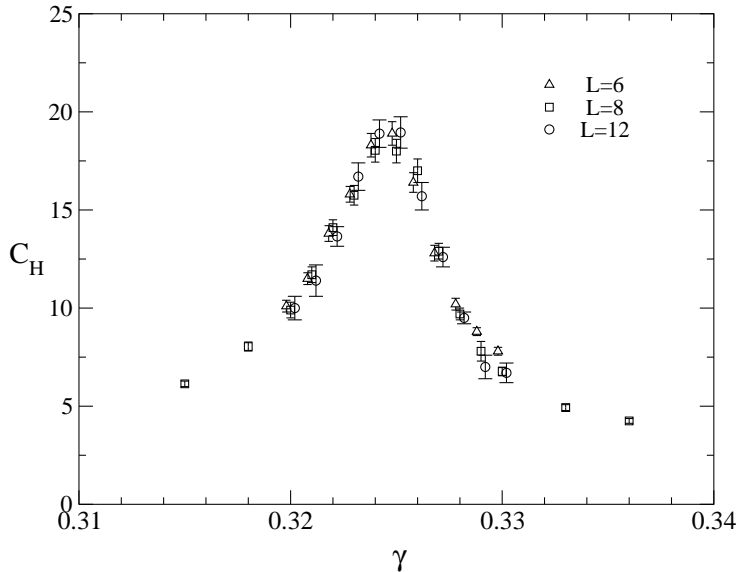


Figure 9: Specific heat versus γ for $SU(4)$ as obtained from simulations on 6^4 , 8^4 and 12^4 lattices. Data for $L = 6, 12$ are slightly shifted horizontally to make the figure more readable.

We mention that early works, based on mean field calculations [47] and Monte Carlo simulations [42, 44], suggested a bulk first-order phase transition also for $SU(4)$ and $\beta \simeq 10.4$. Results confirming the lack of a bulk transition have been recently reported in Ref. [63].

C. Critical slowing down for the topological modes

Monte Carlo simulations of critical phenomena in statistical mechanics and of the continuum limit in quantum field theory are hampered by the problem of critical slowing down. For a general introduction to critical slowing down in Monte Carlo simulations, see e.g. Ref. [64]. The autocorrelation time τ , which corresponds to the number of iterations needed to generate a new independent configuration, grows with increasing length scale ξ ; usually it blows up following a power law, i.e. $\tau \sim \xi^z$. In gauge theories one may consider $\xi_\sigma \equiv \sigma^{-1/2}$ as a length scale. Critical slowing down for traditional algorithms, such as standard Metropolis or heat bath, arises essentially from the fact that their updating is local: in a single step of the algorithm, information is transmitted from a given site/link to the nearest neighbors. Roughly, one expects that this information spreads following a random walk around the lattice. An essentially independent configuration is obtained when the information travels a distance of the order of the correlation length ξ . This suggests that

$\tau \sim \xi^2$. This guess is correct for Gaussian (free field) models; in general one expects that $\tau \sim \xi^z$ where z is a dynamical critical exponent. In the case of local algorithms, such as Metropolis and heat bath, one expects $z \simeq 2$. Appropriate overrelaxation procedures may achieve a reduction of z , although the condition $z \geq 1$ holds for local algorithms. On the other hand, in the presence of relevant topological modes, the random-walk picture may fail. These modes may give rise to sizeable free-energy barriers separating different regions of the configuration space. The evolution in the configuration space may present a long-time relaxation due to transitions between different topological charge sectors. (Although lattice field theories cannot strictly possess topological properties, these are expected to be recovered in the continuum limit.) As in glass models, see e.g. Ref. [65], and in liquids below a crossover transition, see e.g. Ref. [66], the presence of significant free-energy barriers may determine an effective separation of short-time relaxation within the free-energy basins from long-time relaxation related to the transitions between basins. The mechanism underlying this long-time relaxation is rather different from the simple random-walk spread of information, so the autocorrelation time of the topological modes may not show a simple power law behavior. This picture was also behind the so-called heating method [67] to measure the lattice renormalizations of topological charge operators. This method exploits the critical slowing down of the physical topological modes in off-equilibrium simulations, to disentangle them from the short-distance lattice renormalizations.

Let us consider an observable O ; its autocorrelation function $C_O(t)$ (t is the Monte Carlo time, i.e. the integer counting Monte Carlo iterations at equilibrium) is defined as

$$C_O(t) = \langle (O(t) - \langle O \rangle) (O(0) - \langle O \rangle) \rangle, \quad (\text{C.1})$$

where the averages are taken at equilibrium. The integrated autocorrelation time τ_O associated with O is given by

$$\tau_O = \frac{1}{2} \sum_{t=-\infty}^{t=+\infty} \frac{C_O(t)}{C_O(0)}. \quad (\text{C.2})$$

Estimates of τ_O can be obtained by a blocking analysis of the data, without measuring the autocorrelation function $C_O(t)$. Indeed the following relation holds

$$\tau_O = N_m \frac{E^2}{2E_0^2}, \quad (\text{C.3})$$

where N_m is the number of sweeps between two measurements of the observable O , E_0 is the naive error calculated without taking into account the autocorrelations, and E is the correct error found after the blocking procedure (the estimate is meaningful only if $N_m \lesssim \tau_O$). Of course τ_O depends on the observable O ; the largest value τ_O among the various observables provides the time scale to obtain a new independent

configuration in simulations at equilibrium. In Ref. [68] the autocorrelation time τ_w of small Wilson loops was found to behave approximately as $\tau_w \sim \xi^2$ for the SU(3) gauge theories, see also Ref. [69]. As we shall see, a more severe form of critical slowing down is observed in measuring quantities related to the topological modes, such as the topological charge Q .

We used cooling to determine Q from each lattice configuration, measuring Q every $N_m = 100$ Monte Carlo sweeps. Estimates of the (integrated) autocorrelation time τ_Q were obtained by a blocking analysis of the data, using Eq. (C.3). In the SU(6) case we found $\tau_Q \approx 268$ for $\gamma = 0.342$, $\tau_Q \approx 466$ for $\gamma = 0.344$, $\tau_Q \approx 1750$ for $\gamma = 0.348$, and $\tau_Q \gtrsim 3000$ for $\gamma = 0.350$. Moreover we found that the run at the largest value of γ considered, i.e. $\gamma = 0.354$, did not correctly sample the topological charge presumably because the expected τ_Q is large and the run was not sufficiently long (approximately 300k sweeps). In the SU(4) case we found $\tau_Q \approx 101$ for $\gamma = 0.338$, $\tau_Q \approx 210$ for $\gamma = 0.341$, and $\tau_Q \approx 410, 434$ for $\gamma = 0.344$ and $L = 16, 12$. The uncertainty on the above numbers should be at most 5% for SU(4) and 10-20% for SU(6).

These estimates of τ_Q are suggestive of an interesting phenomenon. As shown in Fig. 10, they are consistent with an exponential critical slowing down. Indeed the data for the autocorrelation time can be well fitted by an exponential behavior of the type $\tau_Q \propto \exp(c\xi_\sigma)$ with $c \approx 2.5$ for SU(6) and $c \approx 1.7$ for SU(4). One might also guess an increase of the constant c according to $c \sim N$. We also mention that the data for τ_Q are definitely inconsistent with a behavior of the type ξ_σ^z with $z \simeq 2$. Indeed, an acceptable power law behavior fitting reasonably well the data for τ_Q would require $z \simeq 7$ for SU(4) and $z \simeq 9$ for SU(6). We expect that a similar critical slowing down phenomenon occurs also for SU(3), and more generally in the presence of dynamical fermions.

This dramatic effect was not observed for the other quantities considered in our study, such as the correlations determining the k -string tensions and the glueball masses. A blocking analysis of the data did not show significant time correlations in measurements taken every 10-20 sweeps for all values of γ considered. For instance, in the case of SU(4) and for $\gamma = 0.344$ and $L = 16$ the autocorrelation time τ_P of smeared and blocked Polyakov line correlators was estimated to be smaller than 10, more precisely $\tau_P \approx 6$, by a blocking analysis of the data. This fact suggests an approximate decoupling between the topological and nontopological modes. This seems to be also supported by the fact that string tension results for $\gamma = 0.354$ in the SU(6) case (see Table 4), extracted from a simulation which did not sample correctly Q , turn out to be in agreement with those for smaller γ , for which Q was sampled correctly.

Such a critical slowing down phenomenon was already observed in simulations of two-dimensional CP^{N-1} models [70, 71]. Given that these models possess some of the properties expected to hold in QCD [72, 73] (asymptotic freedom, a form of confine-

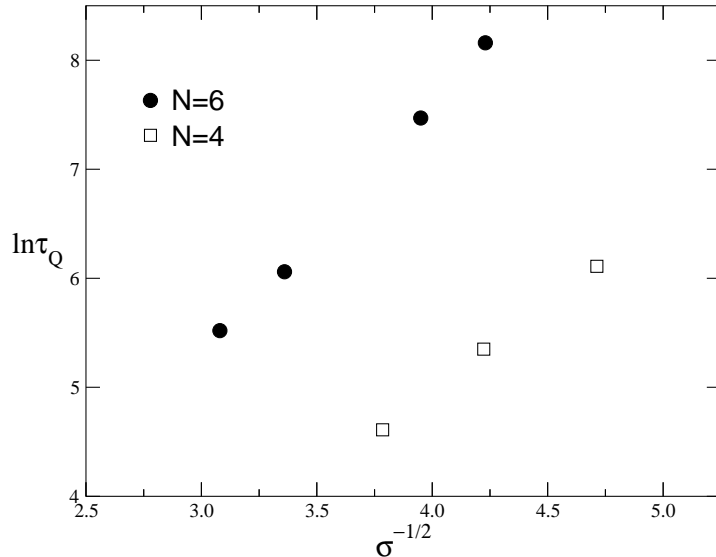


Figure 10: Plot of the autocorrelation time τ_Q of the topological charge versus $\sigma^{-1/2}$.

ment due to the $U(1)$ gauge invariance, a nontrivial topological structure), they have been used as a laboratory to check and develop methods to investigate topological properties. Monte Carlo studies of lattice formulations of two-dimensional CP^{N-1} models, using local algorithms (mixtures of overrelaxation and heat bath upgradings, similar to the ones generally used for the four-dimensional $SU(N)$ gauge theories), have shown that the critical slowing down of the topological modes is consistent with an exponential growing with respect to the correlation length, worsening with increasing N . On the other hand, nontopological quantities, such as the mass gap and Wilson loops, turned out not to be affected by this problem, suggesting a large decoupling between the topological and nontopological modes.

References

- [1] G. 't Hooft, *Nucl. Phys.* **B 72** (1974) 461.
- [2] S. R. Das, *Rev. Mod. Phys.* **59** (1987) 235.
- [3] A. M. Polyakov, *Gauge Fields and Strings*, Harwood Academic Publishers, New York 1988.
- [4] P. Rossi, M. Campostrini, and E. Vicari, *Phys. Rept.* **302** (1998) 143.
- [5] A. Manohar, e-print [hep-ph/9802419](https://arxiv.org/abs/hep-ph/9802419).

- [6] M. J. Strassler, *Prog. Theor. Phys. Suppl.* **131** (1998) 439, [e-print hep-th/9803009]; *Nucl. Phys.* **73** (*Proc. Suppl.*) (1999) 120, [e-print hep-lat/9810059].
- [7] M. Lüscher, K. Symanzik, and P. Weisz, *Nucl. Phys.* **B 173** (1980) 365.
- [8] M. Caselle, R. Fiore, F. Gliozzi, M. Hasenbusch, and P. Provero, *Nucl. Phys.* **B 486** (1997) 245.
- [9] M. R. Douglas and S. H. Shenker, *Nucl. Phys.* **B 447** (1995) 271.
- [10] A. Hanany, M. J. Strassler, and A. Zaffaroni, *Nucl. Phys.* **B 513** (1998) 87.
- [11] C.P. Herzog and I.R. Klebanov, e-print hep-th/0111078.
- [12] E. Witten, *Nucl. Phys.* **B 500** (1997) 3; *Nucl. Phys.* **B 507** (1997) 658.
- [13] J. Ambjorn, P. Olesen, and C. Peterson, *Nucl. Phys.* **B 240** (1984) 533.
- [14] J. B. Kogut and L. Susskind, *Phys. Rev.* **D 11** (1975) 395.
- [15] J. B. Kogut, *Rev. Mod. Phys.* **55** (1983) 775.
- [16] M. Creutz, *Quarks, Gluons and Lattices* (Cambridge University Press, Cambridge, 1985).
- [17] M. Peter, *Phys. Rev. Lett.* **78** (1997) 602; *Nucl. Phys.* **B 501** (1997) 471.
Y. Schröder, *Phys. Lett.* **B 447** (1999) 321.
- [18] V. I. Shevchenko and Yu. A. Simonov, *Phys. Rev. Lett.* **85** (2000) 1811; e-print hep-ph/0104135.
- [19] B. Lucini and M. Teper, *Phys. Lett.* **B 501** (2001) 128; *Phys. Rev.* **D 64** (2001) 105019; e-print hep-lat/0110004.
- [20] Y. Koma, E. Ilgenfritz, H. Toki, and T. Suzuki, *Phys. Rev.* **D 64** (2001) 011501(R).
- [21] M. Faber, J. Greensite, and Š. Olejník, *Phys. Rev.* **D 57** (1998) 2603.
- [22] G. Bali, *Phys. Rev.* **D 62** (2000) 114503.
- [23] S. Deldar, *Phys. Rev.* **D 62** (2000) 034509.
- [24] M. Wingate and S. Ohta, *Phys. Rev.* **D 63** (2001) 094502.
- [25] L. Del Debbio, M. Faber, J. Greensite, Š. Olejník, *Phys. Rev.* **D 55** (1997) 2298.
- [26] J. Heo and T. Vachaspati, *Phys. Rev.* **D 58** (1998) 065011.
- [27] F.A. Schaposnik and P. Suranyi, *Phys. Rev.* **D 62** (2000) 125002.
- [28] A. Yung, e-print hep-th/0005088.

- [29] J. D. Edelstein, W. Garcia Fuertes, J. Mas and J. M. Guilarte, *Phys. Rev. D* **62** (2000) 065008.
- [30] M. A. C. Kneipp and P. Brockill, e-print [hep-th/0104171](#), *Phys. Rev. D* in press.
- [31] S. Deldar, *J. High Energy Phys.* **0101** (2001) 013.
- [32] K. Konishi and L. Spanu, e-print [hep-th/0106175](#).
- [33] J. Shigemitsu and J. B. Kogut, *Nucl. Phys. B* **190** (1981) 365.
- [34] E. Abdalla, M. C. B. Abdalla, and A. Lima-Santos, *Phys. Lett. B* **104** (1984) 71.
- [35] P. Wiegmann, *Phys. Lett. B* **141** (1984) 173; *Phys. Lett. B* **141** (1984) 217.
- [36] L. Del Debbio, H. Panagopoulos, P. Rossi, and E. Vicari, *Phys. Rev. D* (Rap. Comm.) in press, e-print [hep-th/0106185](#).
- [37] L. Del Debbio, H. Panagopoulos, P. Rossi, and E. Vicari, e-print [hep-lat/0110101](#).
- [38] N. Cabibbo and E. Marinari, *Phys. Lett. B* **119** (1982) 387.
- [39] G. Parisi, in *High Energy Physics 1980*, Proceedings of the XXth Conference on High Energy Physics, Madison, 1980, edited by L. Durand and L. G. Pondrom, AIP Conf. proc. No. 68 (AIP, New York 1981).
- [40] G. P. Lepage and P. B. MacKenzie, *Phys. Rev. D* **48** (1993) 2250.
- [41] H. Panagopoulos and E. Vicari, *Phys. Rev. D* **58** (1998) 114501; *Phys. Rev. D* **59** (1999) 057503; *Nucl. Phys.* **83-84** (*Proc. Suppl.*) (2000) 884.
- [42] M. Creutz, *Phys. Rev. Lett.* **46** (1981) 1441.
- [43] M. Creutz and K. J. M. Moriarty, *Phys. Rev. D* **25** (1982) 1724.
- [44] K. J. M. Moriarty, *Phys. Lett. B* **106** (1981) 130.
D. Barkai, M. Creutz, and K. Moriarty, *Nucl. Phys. B* **225** (1983) 156.
G. G. Batrouni and B. Svetitsky, *Phys. Rev. Lett.* **52** (1984) 2205.
- [45] S. Itoh, Y. Iwasaki, and T. Yoshié, *Phys. Rev. Lett.* **55** (1995) 273.
- [46] J.-M. Drouffe and J.-B. Zuber, *Phys. Rept.* **102** (1983) 1.
- [47] C. Itzykson and J. Drouffe, *Statistical field theory* (Cambridge University Press, Cambridge, 1989).
- [48] M. Campostrini, *Nucl. Phys.* **73** (*Proc. Suppl.*) (1999) 724 [e-print [hep-lat/9809072](#)].
- [49] B. Lucini and M. Teper, *J. High Energy Phys.* **0106** (2001) 050.
- [50] M. Teper, *Nucl. Phys.* **83** (*Proc. Suppl.*) (2000) 146 [e-print [hep-lat/9909124](#)].

- [51] P. de Forcrand, G. Schierholz, H. Schneider, and M. Teper, *Phys. Lett.* **B 160** (1985) 137.
- [52] M. Teper, e-print [hep-th/9812187](#).
- [53] M. Teper, *Phys. Lett.* **B 183** (1987) 345.
M. Albanese et al. (APE Collaboration), *Phys. Lett.* **B 192** (1987) 163.
- [54] J. B. Kogut, R. B. Pearson, and J. Shigemitsu, *Phys. Rev. Lett.* **43** (1979) 484.
J. B. Kogut and J. Shigemitsu, *Phys. Rev. Lett.* **45** (1980) 410.
- [55] F. Green and S. Samuel, *Nucl. Phys.* **B 190** (1981) 113.
- [56] P. Rossi, *Ann. Phys. (NY)* **132** (1981) 463.
- [57] A. A. Migdal, *J. E. T. P.* **42** (1975) 743.
- [58] P. Rossi and E. Vicari, *Phys. Rev.* **D 49** (1994) 1621; *Phys. Rev.* **D 49** (1994) 6072;
(E) *Phys. Rev.* **D 55** (1997) 1698.
- [59] I. T. Drummond and R. R. Horgan, *Phys. Rev.* **B 327** (1994) 107.
- [60] A. McKane and M. Stone, *Nucl. Phys.* **B 163** (1980) 169.
- [61] M. Teper, *Phys. Lett.* **B 397** (1997) 223.
- [62] M. S. S. Challa, D. P. Landau, and K. Binder, *Phys. Rev.* **B 34** (1986) 1841.
- [63] R. V. Gavai, e-print [hep-lat/0110054](#).
- [64] A. D. Sokal, in *Quantum Fields on the Computer*, ed. M. Creutz (World Scientific, Singapore, 1992).
- [65] G. Parisi. *Nucl. Phys.* **26 (Proc. Suppl.)** (1992) 181.
- [66] T. B. Schroder, S. Sastry, J. D. Dyre, and C. Glotzer, *J. Chem. Phys.* **112** (2000) 9834.
- [67] A. Di Giacomo and E. Vicari, *Phys. Lett.* **B 275** (1992) 429.
- [68] K. Akemi, et al., QCD-TARO Collaboration, *Nucl. Phys.* **34 (Proc. Suppl.)** (1994) 789.
- [69] B. Gehrman and U. Wolff, *Nucl. Phys.* **83 (Proc. Suppl.)** (2000) 801 [e-print [hep-lat/9908003](#)].
- [70] M. Campostrini, P. Rossi, and E. Vicari, *Phys. Rev.* **D 46** (1992) 2647; *Phys. Rev.* **D 46** (1992) 4643.
- [71] E. Vicari, *Phys. Lett.* **B 309** (1993) 139.
- [72] A. D’Adda, P. Di Vecchia, and M. Lüscher, *Nucl. Phys.* **B 146** (1979) 63.
- [73] E. Witten, *Nucl. Phys.* **B 149** (1979) 285.